

A new rotating black hole from the Newman-Janis algorithm

Hyeong-Chan Kim^{¶1}, Wonwoo Lee^{§2}

¶*School of Liberal Arts and Sciences, Korea National University of Transportation, Chungju 27469, Korea*

§*Center for Quantum Spacetime, Sogang University, Seoul 04107, Korea*

Abstract

We present a new rotating black hole solution to the Einstein equations as an extension of the Kerr spacetime. To derive this solution, we use the Newman-Janis algorithm as a mathematical tool that reduces a general rotating metric into a tractable form by applying simple physical requirements. Interestingly, the solution we found may not be uniquely characterized by asymptotic parameters such as mass, angular momentum, and charge, thereby challenging the no-hair theorem. We also analyze in detail how this additional characteristics (“hair”) affects the thermodynamic properties of the black hole.

¹*email: hckim@ut.ac.kr*

²*email: warrior@sogang.ac.kr*

1 Introduction

The study of black holes has made significant progress, particularly following their indirect detections [1, 2, 3, 4, 5, 6, 7] not only provide a deeper understanding of various astrophysical phenomena but also serve as an intriguing subject of theoretical investigation. In particular, static, spherically symmetric black holes offer an idealized framework for analyzing complex gravitational systems. Once these simpler models are well understood, the insights gained can pave the way for studying rotating black holes. However, this transition poses considerable challenges due to the increased complexity of the equations governing their geometry. The computational demands of studying rotating black holes often necessitate simplifications, such as assuming axial symmetry or focusing on static cases.

A key solution describing a rotating black hole in vacuum is the Kerr metric [8], serves as a foundational reference for deriving more general rotating black hole solutions that incorporate matter fields. The Kerr solution provides a remarkably accurate description of astrophysical black holes and is widely accepted as the best approximation for rotating black holes in the Universe. However, real black holes in galaxies exist in environments filled with dark matter and dark energy. Thus, it is necessary to explore more general solutions that take into account the effects of a cosmological constant and matter fields. Studying such extensions can offer deeper insights into the dynamics and observational signatures of astrophysical black holes.

This naturally raises the question: How can we derive solutions for rotating black holes that coexist with surrounding matter fields? The first major extension in this direction was the Kerr-Newman solution [9], which describes a rotating, charged black hole in Einstein-Maxwell theory. This solution was derived using the Newman-Janis (NJ) algorithm [10], a method that has been widely studied and debated [11, 12, 13]. While the underlying reason how the algorithm works remains unclear, its empirical success makes it a valuable tool for deriving rotating black hole solutions. Recent research has focused on extending this algorithm to incorporate additional matter fields [14, 15, 16, 17]. There is also considerable interest in which types of fields can coexist with rotating black holes while maintaining physical consistency [18, 19, 17]. In various theories of gravity, efforts have been made new rotating black hole solutions in different spacetime dimensions [20, 21, 22, 23, 24, 25, 26, 27].

To study the matter fields coexisting with a rotating black hole, it is crucial to analyze the components of the stress-energy tensor and understand the equation of state, which determines the nature of the matter [28]. Such an analysis provides valuable insights into the behavior of the matter fields surrounding the rotating black holes. For the electrically charged Kerr-Newman black hole, the stress-energy tensor reveals that the energy density is related to the radial pressure by the equation of state $\varepsilon = -p_r$. Interestingly, Maxwell's field having this property does not behave as a perfect fluid. When considering more general matter fields, two main approaches emerge: First is to find a rotating black hole solution that coexists with matter of the perfect fluid type [29, 30]. The second involves extending the Kerr-(Newman) black hole to the rotating black hole with matter fields having the property $\varepsilon = -p_r$, such as electric fields [31, 32, 33, 34, 35, 36, 37, 38, 39, 40, 41].

The no-hair theorem is well-established for the electrovacuum solution of Einstein-Maxwell theory [64], which states that black holes are characterized solely by their mass, charge, and angular momentum as primary hairs. However, in Einstein-Maxwell theory with additional matter fields beyond ordinary matter or in extensions of general relativity, the applicability of the no-hair theorem is not necessarily evident. When fields other than the electromagnetic field are present, additional hairs may emerge. In the Einstein-scalar theory with minimal coupling, Bekenstein’s no-hair theorem holds under the assumption that the energy density of the scalar field outside the black hole horizon is non-negative [42, 43]. Thus, the theorem can be circumvented if this assumption is violated [44, 45, 46, 47, 48, 49, 50, 51]. Further investigation is required to determine whether such hair should be classified as primary or secondary [52, 53, 54].

Rather than following the conventional classification, in this work, we categorize black hole hairs in general relativity into two types based on their effect on the geometry, a distinction that is useful for our later discussion. The first type of hair directly modifies the metric, meaning its presence alters the stress-energy tensor. This category includes conventional hairs such as mass, charge, and angular momentum, as well as most non-Abelian and dilatonic hairs. The second type of hair, in contrast, does not affect the metric but can still be detected through global measurements, such as Aharonov-Bohm-type scattering [55]. Examples include axionic quantum hair and discrete gauge charges. Interestingly, stress-energy tensors associated with the first type of hair typically decay polynomially at large distances, making their influence detectable by asymptotic observers. This observation raises an intriguing question: Could there exist a new type of black hole hair that remains undetectable to an asymptotic observer yet can be identified through local measurements? For such a hair to exist, its associated stress-energy tensor must be bounded near the event horizon and decay no slower than exponentially at large distances.

In this work, we explore the Newman-Janis algorithm in a general setting and analyze its role in constructing rotating black hole geometries that coexist with matter fields. Our approach extends beyond the standard Kerr-Newman solution, allowing for more general modifications allowing the new kind of hairs while maintaining physical consistency. We investigate the structure of these solutions and discuss their implications for black hole physics and astrophysical observations.

The paper is organized as follows: In Secs. 2 and 3, we investigate the mathematical structure of the NJ algorithm more closely and derive a new solution, which is a generalization of the Kerr black hole coexisting with a matter field. Sec. 4 is dedicated to analyzing the properties of this new solution in depth. In Sec. 5, we explore the implications of the new solution for black hole thermodynamics, with a focus on how the presence of the new matter field affects thermodynamic properties. Finally, we summarize our findings and discuss their broader implications in the concluding section.

2 Mathematical structure of the Newman-Janis algorithm

In this section, we revisit and analyze the mathematical structure of the NJ algorithm in a general setting. The goal is to provide a detailed mathematical analysis of the original NJ algorithm to derive a new solution corresponding to a rotating black hole geometry. To ensure that the resulting metric describes physical spacetime, it is necessary to verify that the metric satisfies the Einstein equation and derive the corresponding energy-momentum tensor, which will be done in the next section. Throughout this analysis, we assume that the spacetime geometry is asymptotically flat.

As the base geometry, we consider a static, spherically symmetric metric of the form,

$$ds^2 = -f(r)dt^2 + \frac{dr^2}{g(r)} + \sigma(r)d\Omega^2, \quad (1)$$

where $d\Omega^2 = d\theta^2 + \sin^2\theta d\phi^2$ represents the angular part of the metric. When $\sigma(r) = r^2$, the radial coordinate r corresponds to the areal radius. However, if $\sigma(r) \neq r^2$, the areal radius becomes $\sqrt{\sigma(r)}$. At this stage, we do not presume any specific forms for the functions $f(r)$, $g(r)$, and $\sigma(r)$ aside from the asymptotic flatness condition, which requires $f(r), g(r) \rightarrow 1$ and $\sigma(r) \rightarrow r^2$ as $r \rightarrow \infty$.

Let us apply the Newman-Janis algorithm step by step.

1. The first step involves expressing the metric in null coordinates and constructing the corresponding tetrad. We introduce the null coordinate u via the transformation, $du = dt - \frac{dr}{\sqrt{f(r)g(r)}}$, which allows us to rewrite the metric (1) in the Eddington-Finkelstein form:

$$ds^2 = -f(r)du^2 - 2\sqrt{\frac{f(r)}{g(r)}}dudr + \sigma(r)d\Omega^2. \quad (2)$$

Next, we construct a set of tetrads $\{l_\mu, n_\mu, m_\mu, \bar{m}_\mu\}$ satisfying the pseudo-orthogonality relations: $l^\mu n_\mu = -1$ and $m^\mu \bar{m}_\mu = 1$, with the metric expressed as:

$$g_{\mu\nu} = -l_\mu n_\nu - n_\mu l_\nu + m_\mu \bar{m}_\nu + \bar{m}_\mu m_\nu. \quad (3)$$

The components of the tetrad are then given by

$$\begin{aligned} l_\mu &= \delta_\mu^0, & n_\mu &= \frac{f(r)}{2}\delta_\mu^0 + \sqrt{\frac{f(r)}{g(r)}}\delta_\mu^1, \\ m_\mu &= \frac{\sqrt{\sigma(r)}}{\sqrt{2}}(\delta_\mu^2 + i \sin\theta \delta_\mu^3), & \bar{m}_\mu &= \frac{\sqrt{\sigma(r)}}{\sqrt{2}}(\delta_\mu^2 - i \sin\theta \delta_\mu^3). \end{aligned} \quad (4)$$

It is straightforward to verify that this tetrad satisfies the required conditions. The tetrad components with upper indices can be computed as:

$$l^\mu = -\sqrt{\frac{g(r)}{f(r)}}\delta_1^\mu, \quad n^\mu = \left(-\delta_0^\mu + \frac{\sqrt{f(r)g(r)}}{2}\delta_1^\mu\right), \quad m^\mu = \frac{1}{\sqrt{2\sigma(r)}}\left(\delta_2^\mu + \frac{i}{\sin\theta}\delta_3^\mu\right). \quad (5)$$

This tetrad construction forms the foundation for the application of the NJ algorithm to derive the rotating solution.

2. The second step involves performing a complex coordinate transform from $(u, r) \rightarrow (u', r')$ ³ as follows:

$$u' = u - iap(x), \quad r' = r + iaq(x), \quad x = \cos\theta, \quad (6)$$

where a denotes the rotation parameter. The angle dependent functions $p(x)$ and $q(x)$ denote distinct coordinates transforms for u and r . Notably, we do not assume $p(x) = q(x)$ in general. Later in this work, we find $p(x) = q(x)$ for the Schwarzschild case, dictated by physical requirements rather than purely mathematical reasons.

In this new coordinates, $x^\mu = (u', r', \theta, \phi)$, the tetrad vectors are expressed as:

$$\begin{aligned} l^\mu &= -\sqrt{\frac{G(r, \theta)}{F(r, \theta)}}\delta_1^\mu, \\ n^\mu &= -\delta_0^\mu + \frac{\sqrt{F(r, \theta)G(r, \theta)}}{2}\delta_1^\mu, \\ m^\mu &= \frac{1}{\sqrt{2\Sigma(r, \theta)}}\left[ia\sin\theta(\dot{p}(x)\delta_0^\mu - \dot{q}(x)\delta_1^\mu) + \delta_2^\mu + \frac{i}{\sin\theta}\delta_3^\mu\right], \end{aligned} \quad (7)$$

where $\dot{p}(x) \equiv (dp(x)/dx)$ and $\dot{q} \equiv (dq(x)/dx)$. Here, $F(r, \theta)$, $G(r, \theta)$, and $\Sigma(r, \theta)$ represent generalizations of the functions $f(r)$, $g(r)$, and $\sigma(r)$ in the presence of the rotation parameter a , respectively. In performing this generalization, one usually adopt the prescriptions

$$r^2 \rightarrow (r + iaq)(r - iaq), \quad \frac{2}{r} \rightarrow \frac{1}{r + iaq} + \frac{1}{r - iaq}. \quad (8)$$

However, as noted in Ref. [11], ambiguities arise in applying these prescriptions, particularly in the second case. These ambiguities cannot be fully resolved by mathematical reasoning alone and are addressed using physical arguments in the next section.

Using the tetrad, we reconstruct the inverse metric from the relation $-l^\mu n^\nu - n^\mu l^\nu + m^\mu \bar{m}^\nu + \bar{m}^\mu m^\nu = g^{\mu\nu}$. Inverting the inverse metric yields the line elements in the new

³In the original form, $p(x) = q(x) = x = \cos\theta$. More general transform could be assumed as in Ref. [11].

coordinates (u', r', θ, ϕ) :

$$\begin{aligned}
ds^2 = & -F(r, \theta) du^2 - 2\sqrt{\frac{F(r, \theta)}{G(r, \theta)}} du dr - 2a \left(\dot{q}(x) \sqrt{\frac{F(r, \theta)}{G(r, \theta)}} - \dot{p}(x) F(r, \theta) \right) \sin^2 \theta du d\phi \\
& + 2a \sqrt{\frac{F(r, \theta)}{G(r, \theta)}} \dot{p}(x) \sin^2 \theta dr d\phi + \Sigma(r, \theta) d\theta^2 \\
& + \left(\Sigma(r, \theta) + \dot{p}(x) \left(2\dot{q}(x) \sqrt{\frac{F(r, \theta)}{G(r, \theta)}} - \dot{p}(x) F(r, \theta) \right) a^2 \sin^2 \theta \right) \sin^2 \theta d\phi^2. \quad (9)
\end{aligned}$$

For simplicity, we omit the primes for the coordinates.

3. The next step in the NJ algorithm is to transform the metric into a rotating form by removing the off-diagonal components $dt dr$ and $dr d\phi$. To achieve this, we introduce the following coordinate transformations:

$$du = dt - \frac{\Gamma(r) dr}{\Delta(r)}, \quad d\phi = d\psi - \frac{a dr}{\Delta(r)}. \quad (10)$$

Since u and ϕ are coordinate bases, the transformations in equation (10) must satisfy the condition of integrability. This implies that the functions $\Gamma(r)$ and $\Delta(r)$ depend only on r and are independent of θ .

This dependency is significant as it greatly simplifies the process of solving the Einstein equation in a rotating system. The integrability condition also ensures that the transformed metric components g_{tr} and $g_{r\psi}$ vanish, as required to describe a stationary rotating solution with a symmetry axis aligned along the z -direction.

To enforce these constraints, the form of $F(r, \theta)$ and $G(r, \theta)$ are determined in terms of $\Delta(r)$ and $\Gamma(r)$ as follows:

$$F(r, \theta) = \frac{\Sigma(r, \theta) (\Delta(r) - a^2 \dot{q}(x) \sin^2 \theta)}{\dot{q}(x) (\Gamma(r) - a^2 \dot{p}(x) \sin^2 \theta)^2}, \quad G(r, \theta) = \frac{\dot{q}(r)}{\Sigma(r, \theta)} [\Delta(r) - \dot{q}(x) a^2 \sin^2 \theta]. \quad (11)$$

With these forms, the metric is transformed into a Boyer-Lindquist form [56]

$$\begin{aligned}
ds^2 = & -F(r, \theta) dt^2 - 2a \left(\dot{q}(x) \sqrt{\frac{F(r, \theta)}{G(r, \theta)}} - \dot{p}(x) F(r, \theta) \right) \sin^2 \theta dt d\psi + \Sigma(r, \theta) d\theta^2 \\
& + \frac{1}{\dot{q}(x)} \frac{\Sigma(r, \theta)}{\Delta(r)} dr^2 \\
& + \left[\Sigma(r, \theta) + a^2 \sin^2 \theta \dot{p}(x) \left(2\dot{q}(x) \sqrt{\frac{F(r, \theta)}{G(r, \theta)}} - \dot{p}(x) F(r, \theta) \right) \right] \sin^2 \theta d\psi^2. \quad (12)
\end{aligned}$$

At this stage, the NJ algorithm formally concludes, providing the general rotating metric. Further analysis, such as checking the Einstein equations and determining the physical implications, is required to finalize the solution.

As demonstrated in the next section, the Kerr and the Kerr-Newman black holes can be derived using the three steps by choosing $p(x) = q(x) = x$ and applying the prescription (8). With the specific choice, the Einstein equation is automatically satisfied. However, in general cases, the metric (12) must independently satisfy the Einstein equations without relying solely on the prescription (8). This opens the possibility of exploring different prescriptions or alternative functional forms for $p(x)$ and $q(x)$, provided the resulting metric (12) remains consistent with the Einstein equation. In the next section, we investigate whether such alternative choices are feasible and physically meaningful.

The determinant of the metric (12) is given by

$$\det g_{\mu\nu} = -\frac{F(r, \theta)\Sigma^2(r, \theta)}{G(r, \theta)} \sin^2 \theta = -\left(\frac{\Sigma^2(r, \theta) \sin \theta}{\dot{q}(x)(\Gamma(r) - a^2\dot{p}(x) \sin^2 \theta)}\right)^2.$$

Note that the coefficient of dr^2 becomes $g_{rr}(r, \theta) = \frac{1}{\dot{q}(x)} \frac{\Sigma(r, \theta)}{\Delta(r)}$. Here, $\Sigma(r, \theta)$ and $\Delta(r)$ are positive-definite asymptotically. To avoid negative values for g_{rr} in the asymptotic region and to prevent an unwanted singularity in $\det g_{\mu\nu}$, we require

$$\dot{q}(x) > 0, \quad \Gamma(r) > |a^2\dot{p}(x)| \quad \text{for all } |x| \leq 1. \quad (13)$$

A typical choice is $\dot{q}(x) = 1$ as the θ -dependence in the g_{rr} term, except for $\Sigma(r, \theta)$, could disrupt the axial symmetry of the system.

We now rewrite this metric to the form of an orthonormal, non-coordinate basis frame. Additionally, we replace the angle $\psi \rightarrow \phi$, yielding

$$\begin{aligned} ds^2 = & -\frac{\Sigma(r, \theta)\Delta(r)}{\dot{q}(x) (\Gamma(r) - \dot{p}(x)a^2 \sin^2 \theta)^2} (dt - \dot{p}(x)a \sin^2 \theta d\phi)^2 \\ & + \Sigma(r, \theta)d\theta^2 + \frac{1}{\dot{q}(x)} \frac{\Sigma(r, \theta)}{\Delta(r)} dr^2 \\ & + \frac{\Sigma(r, \theta) \sin^2 \theta}{(\Gamma(r) - \dot{p}(x)a^2 \sin^2 \theta)^2} (\Gamma(r)d\phi - a dt)^2. \end{aligned} \quad (14)$$

The metric (14) is a mathematical generalization of the general spherically symmetric metric (1) by the Newman-Janis algorithm. In this metric, there are five unknown functions to be determined. Of these, only $\Sigma(r, \theta)$, which generalizes $\sigma(r)$, depends on both r and θ . The coordinate transformation functions $p(x)$ and $q(x)$ are functions of θ only, while $\Gamma(r)$ and $\Delta(r)$ depend only on r . The physical context should specify the appropriate choices for these functions. Rewriting the metric in this form is essential, as the Einstein tensors in this basis, for geometries like the Kerr, Kerr-Newman black holes, take diagonal forms.

Note that the functions $F(r, \theta)$ and $G(r, \theta)$ are the generalization of $f(r)$ and $g(r)$. Therefore, in the non-rotating limit, we have

$$g(r) \equiv \lim_{a \rightarrow 0} G(r, \theta) = \lim_{a \rightarrow 0} \frac{\dot{q}(x)\Delta(r)}{\Sigma(r, \theta)}, \quad f(r) \equiv \lim_{a \rightarrow 0} F(r, \theta) = \lim_{a \rightarrow 0} \frac{\Delta(r)\Sigma(r, \theta)}{\dot{q}(x)\Gamma^2}. \quad (15)$$

Noting $\Sigma(r, \theta) \rightarrow \sigma(r)$, $\dot{q}(x) \rightarrow 1$ in the $a \rightarrow 0$ limit, this relation constrains the functional forms for $\Delta(r)$ and $\Gamma(r)$. Since $\sigma(r)$ is independent of θ , we can conclude that $\dot{q}(x)$ must be independent of x in the non-rotating limit.

3 Rotating geometries from the static spherically symmetric black hole

In this section, we demonstrate how to generate rotating geometries starting from a static one by applying the Newman-Janis (NJ) algorithm, as outlined in the previous section. We begin with the Schwarzschild metric and use the method to construct not only the Kerr geometry but also several new rotating geometries.

The Schwarzschild metric, which describes a static, spherically symmetric black hole, is given by

$$ds^2 = - \left(1 - \frac{2M}{r}\right) dt^2 + \frac{dr^2}{1 - 2M/r} + r^2 d\Omega^2, \quad r \geq 0. \quad (16)$$

For this metric, the associated functions are:

$$f(r) = g(r) = 1 - \frac{2M}{r}, \quad \sigma(r) = r^2.$$

Since the Schwarzschild black hole is a vacuum solution, the Einstein tensor that corresponds to this geometry vanishes, satisfying the Einstein field equations in the absence of any matter. Now, we proceed to develop a rotating geometry step by step using the NJ algorithm.

3.1 The Kerr geometry

To illuminate the procedure, we step through the derivation of the Kerr geometry using the Newman-Janis (NJ) algorithm, starting from the Schwarzschild metric. Here's the process broken down:

1. We begin by choosing the coordinate transformation functions. For simplicity, we set $q(x) = x$, which satisfies the constraint in Eq. (13).
2. The next step is to define the function $\Sigma(r, \theta)$ starting from $\sigma(r) = r^2$. Following the prescription (8), the generalization to $\Sigma(r, \theta)$ appears unambiguous,

$$\Sigma(r, \theta) = (r + iaq)(r - iaq) = r^2 + a^2q^2 = r^2 + a^2 \cos^2 \theta. \quad (17)$$

3. On the other hand, the generalization from $f(r)$ and $g(r)$ to $F(r, \theta)$ and $G(r, \theta)$ requires caution. The reason is that the functions $F(r, \theta)$ and $G(r, \theta)$ should be defined through the functions $\Delta(r)$ and $\Gamma(r)$ indirectly from Eq. (11). From the non-rotating limit in Eq. (15), we know

$$\lim_{a \rightarrow 0} \Delta(r) = r^2 g(r) = r^2 - 2Mr, \quad \lim_{a \rightarrow 0} \Gamma(r) = r^2. \quad (18)$$

In fact, any functions $F(r, \theta)$ and $G(r, \theta)$ satisfying the constraints are acceptable if the result is physically sound. For the case of the Kerr geometry, we follow the prescription (8) for G and using Eq. (11), we have

$$g(r) \rightarrow G(r, \theta) = \frac{\Sigma(r, \theta) - 2Mr}{\Sigma(r, \theta)} = \frac{\Delta(r) - a^2 \sin^2 \theta}{\Sigma(r, \theta)}. \quad (19)$$

This leads to the following expression for $\Delta(r)$:

$$\Delta(r) = \Sigma(r, \theta) + a^2 \sin^2 \theta - 2Mr = r^2 + a^2 - 2Mr. \quad (20)$$

Note that this expression for $\Delta(r)$ is consistent with the non-rotating limit (18). We also follow the prescription (8) for $F(r, \theta)$ and get

$$f(r) \rightarrow F(r, \theta) = 1 - \frac{2Mr}{\Sigma(r, \theta)}. \quad (21)$$

Equating this form with that in Eq. (11), we get

$$\Gamma(r) - a^2 \dot{p}(x) \sin^2 \theta = \Sigma(r, \theta) = r^2 + a^2 \cos^2 \theta \rightarrow \Gamma(r) = r^2 + a^2, \quad \dot{p}(x) = 1. \quad (22)$$

Here, we have used the fact that $\Gamma(r)$ is a function of r only. Note that the function $p(x) = x$ is fixed at this step because of the prescription (8).

Substituting the functions $F(r, \theta)$ and $G(r, \theta)$ into the general form of the metric, we obtain the Kerr geometry in the Boyer-Lindquist coordinates,

$$\begin{aligned} ds^2 &= -\frac{\Delta(r) - a^2 \sin^2 \theta}{\Sigma(r, \theta)} dt^2 - \frac{2(r^2 + a^2 - \Delta(r))}{\Sigma(r, \theta)} a \sin^2 \theta dt d\phi + \Sigma(r, \theta) d\theta^2 \\ &\quad + \frac{\Sigma(r, \theta)}{\Delta(r)} dr^2 + \left[-\frac{\Delta(r)}{\Sigma(r, \theta)} a^2 \sin^2 \theta + \frac{(r^2 + a^2)^2}{\Sigma(r, \theta)} \right] \sin^2 \theta d\phi^2 \\ &= -\frac{\Delta(r)}{\Sigma(r, \theta)} (dt - a \sin^2 \theta d\phi)^2 + \frac{\Sigma(r, \theta)}{\Delta(r)} dr^2 \\ &\quad + \Sigma(r, \theta) d\theta^2 + \frac{\sin^2 \theta}{\Sigma(r, \theta)} ((r^2 + a^2) d\phi - a dt)^2. \end{aligned} \quad (23)$$

4. Finally, the Einstein tensor for this geometry is calculated and found to vanish, as expected for a vacuum solution. However, it is important to be cautious when considering the physical implications of this result. The final step in applying the NJ algorithm often involves ensuring that the geometry satisfies physical conditions, such as regularity at the event horizon. We will present this aspect in the next subsection.

The first three steps are merely a mathematical extension of the Schwarzschild geometry using a complex coordinate transformation. The Kerr geometry emerges solely from this mathematical extension. However, the final step, which involves checking its physical implications, is generally necessary.

3.2 Generalization of the Kerr geometry

In this subsection, we develop *new* rotating solutions, which are a generalization of the Kerr geometry. We aim to find new solutions by modifying the Kerr geometry minimally.

1. To make a minimal change from the Kerr geometry, we choose the angle-dependent coordinates transformation functions, $q(x) = x = p(x)$. For $\Sigma(r, \theta)$, we follow the same form as the Kerr's in Eq. (17).
2. In determining $F(r, \theta)$ and $G(r, \theta)$, we do not follow the standard prescription. The only physical requirement which should be maintained is the limiting condition in Eq. (18). Because the functions still be determined from $\Delta(r)$ and $\Gamma(r)$ as given in Eq. (11). Now, we choose the following general form:

$$\Delta(r) = r^2 + a^2 - 2Mr + v(r), \quad \Gamma(r) \equiv r^2 + \tilde{A}(r) + a^2, \quad (24)$$

where $v(r)$ and $\tilde{A}(r)$ denote the deviations from the Kerr geometry. Now, the metric (14) becomes

$$\begin{aligned} ds^2 = & -\frac{\Sigma(r, \theta)\Delta(r)}{\left(\Sigma(r, \theta) + \tilde{A}(r)\right)^2} (dt - a \sin^2 \theta d\phi)^2 + \frac{\Sigma(r, \theta)}{\Delta(r)} dr^2 + \Sigma(r, \theta) d\theta^2 \\ & + \frac{\Sigma(r, \theta) \sin^2 \theta}{\left(\Sigma(r, \theta) + \tilde{A}(r)\right)^2} (\Gamma(r)d\phi - a dt)^2. \end{aligned} \quad (25)$$

3. In this step, we require the condition that the stress tensor does not have the off-diagonal⁴ $r\theta$ component, $T_{\hat{r}\hat{\theta}} = 0$. This is required for fluids undergoing only a rotational motion about a fixed axis (the z -axis here). This leads to $R_{\hat{r}\hat{\theta}} = 0$ [57]. To calculate the Einstein tensor, we take the orthonormal non-coordinate basis from the metric (25):

$$\begin{aligned} \omega^{\hat{t}} &= \frac{\sqrt{\Sigma(r, \theta)\Delta(r)}}{\Sigma(r, \theta) + \tilde{A}(r)} [dt - a \sin^2 \theta d\phi], \quad \omega^{\hat{r}} = \sqrt{\frac{\Sigma(r, \theta)}{\Delta(r)}} dr, \\ \omega^{\hat{\theta}} &= \sqrt{\Sigma(r, \theta)} d\theta, \quad \omega^{\hat{\phi}} = \frac{\sqrt{\Sigma(r, \theta) \sin \theta}}{\Sigma(r, \theta) + \tilde{A}(r)} [\Gamma(r)d\phi - a dt]. \end{aligned} \quad (26)$$

⁴Note however that this non-vanishing value does not imply the existence of shear viscosity between the two directions. One can find an orthonormal basis which makes this value vanish by rotating r and θ directions.

Starting from this basis, we construct the connection 1-form through $d\omega^{\hat{a}} = -\omega^{\hat{a}}_{\hat{b}} \wedge \omega^{\hat{b}}$ and find the curvature 2-form, $\mathfrak{R}^{\hat{a}}_{\hat{b}} = d\omega^{\hat{a}}_{\hat{b}} + \omega^{\hat{a}}_{\hat{c}} \wedge \omega^{\hat{c}}_{\hat{b}}$. From the coefficients of this curvature 2-forms, we read off the curvature components. After a lengthy calculation, one may find that the $r\theta$ component of the Ricci tensor is given by

$$R_{\hat{r}\hat{\theta}} = \frac{3a^2 \sin \theta \cos \theta \sqrt{\Delta(r)} \left(\Sigma^2(r, \theta) \tilde{A}'(r) - 4r \Sigma(r, \theta) \tilde{A}(r) - 2r \tilde{A}^2(r) \right)}{\Sigma^3(r, \theta) \left(\Sigma(r, \theta) + \tilde{A}(r) \right)^2}. \quad (27)$$

Notice that if this tensor does not vanish, it presents the non-vanishing off-diagonal stress tensor $T_{\hat{r}\hat{\theta}}$. Therefore, we choose $R_{\hat{r}\hat{\theta}} = 0$, which leads

$$\tilde{A}(r) = 0 \quad \rightarrow \quad \Gamma(r) = r^2 + a^2. \quad (28)$$

Taking this value, the metric now becomes

$$ds^2 = -\frac{\Delta(r)}{\Sigma(r, \theta)} (dt - a \sin^2 \theta d\phi)^2 + \frac{\Sigma(r, \theta)}{\Delta(r)} dr^2 + \Sigma(r, \theta) d\theta^2 + \frac{\sin^2 \theta}{\Sigma(r, \theta)} [(r^2 + a^2) d\phi - a dt]^2, \quad (29)$$

where $\Delta(r) = r^2 + a^2 - 2Mr + v(r)$ as shown in Ref. [17]. Notice that the metric has almost the same form as the Kerr one except that the function $\Delta(r)$ now includes a correction term, $v(r)$.

4. Finally, we check the Einstein tensor for this geometry (29). The Einstein tensor for this geometry with respect to the basis (26) with $\tilde{A}(r) = 0$ takes the diagonal form:

$$G_{\hat{t}\hat{t}} = -G_{\hat{r}\hat{r}} = \frac{v(r) - rv'(r)}{\Sigma^2(r, \theta)}, \quad G_{\hat{\theta}\hat{\theta}} = G_{\hat{\phi}\hat{\phi}} = \frac{\Sigma(r, \theta)v''(r)/2 + v(r) - rv'(r)}{\Sigma^2(r, \theta)}. \quad (30)$$

Now, let us display a few important cases of the metric. As seen from the value of the Einstein tensor, the geometry is no longer a vacuum solution except for specific choices of v . Note, however, that the developed Einstein tensor vanishes when $v \rightarrow 0$. Also, the equation of state for the radial part $w_r \equiv p_r/\rho = -1$, is always satisfied, which resembles that of the electro-magnetic field for the Kerr-Newman solution. This is satisfied when $f(r) = g(r)$, in which the radial pressure could be the negative of the energy density [58].

5. Note that the two limits $a \rightarrow 0$ and $v(r) \rightarrow 0$ are independent. Therefore we can take the $a \rightarrow 0$ limit with $v(r) \neq 0$. In this case, the metric (29) provides a new static black hole geometry:

$$ds^2 = -\frac{\Delta(r)}{r^2} dt^2 + \frac{r^2}{\Delta(r)} dr^2 + r^2 d\Omega_{(2)}^2, \quad (31)$$

where $\Delta = r^2 - 2Mr + v(r)$. The source developing this metric satisfies $T_{ab} = G_{ab}/8\pi$ with the Einstein tensor given in Eq. (30). Therefore, we interpret that the metric (29) describes the rotating geometry of this static one.

When we choose

$$v(r) = c_1 r + K r^{2-2w}, \quad (32)$$

the metric describes a static black hole made of matter with equation of state $w_\theta = w_\phi = w$ with $w_r = -1$ known in Ref. [40]. Since the c_1 term represents mass rescaling, we set $c_1 = 0$. Now,

$$v(r) - r v'(r) = K(2w - 1)r^{2-2w}.$$

Therefore the positive energy condition holds when

$$K(2w - 1) > 0.$$

6. Let us display a few properties of the solution for various special cases.

- When $v(r) = r v'(r)$, i.e., $v(r) = v_1 r$ is linear in r , the Einstein tensor vanishes. The solution describes the Kerr solution with modified mass $M' = M + v_1/2$.
- When $v(r) = v_0 + v_1 r$, the equation of state takes the form, $w_1 = -1$, $w_2 = w_3 = 1$, which is the same as that of the electro-magnetic field. Therefore, the geometry takes the same form as the Kerr-Newman solution with mass $M' = M + v_1/2$ and the charge squared, $Q^2 = v_0$.
- When $v(r) = v_2 r^2$, the equation of state becomes $w_1 = -1$ and $w_2 = w_3 = -a^2 \sin^2 \theta / r^2$. The energy density $\rho = T^{\hat{t}\hat{t}} = G^{\hat{t}\hat{t}}/8\pi = (-v_2 r^2)/\Sigma^2(r, \theta)$. To interpret this solution, we first consider the $a = 0$ case. Noting the metric (31), we find that the static metric reproduces the global monopole spacetime. Therefore, we can conclude that the solutions with $a \neq 0$ is the rotating global monopole [59].
- When $v(r)$ is given by Eq. (32), the metric (29) describes the rotating geometry of the static solution (31). The equation of state in this case is $w_r = -1$ and $w_\theta = w_\phi = (w-1)\Sigma(r, \theta)/r^2 + 1$. Note that, from the form of the Einstein tensor (30), the angle dependence of the equation of state is unavoidable unless $v''(r) = 0$.
- When $v''(r) = v_c(v(r) - r v'(r))$, i.e.,

$$v(r) = v_1 r + v_2 \left[e^{-v_c r^2/2} + \sqrt{\frac{\pi v_c r^2}{2}} \left(\operatorname{erf} \left(\sqrt{\frac{v_c r^2}{2}} \right) - 1 \right) \right], \quad (33)$$

where $\operatorname{erf}(x)$ denotes the error function, the equation of state becomes $w_1 = -1$, and $w_2 = w_3 = 1 + v_c \Sigma(r, \theta)/2$. This is an interesting generalization of the Kerr family with a minor modification of the equation of state. Note that $v(r) - r v'(r) = v_2 e^{-v_c r^2/2}$. Therefore, the stress tensor exponentially decreases with r . We analyze the properties of the solution in the next section.

- Else, the equation of state for the radial part satisfies $w_1 = -1$. But, $w_2 = w_3$ has an angle dependence. The geometry still describes a stationary rotating black hole with surrounding matter.

As demonstrated in this work, the NJ algorithm does not fully determine the geometry of the system, but rather leaves room for imposing physical requirements. It determines the geometry up to Eq. (25). The final form of the metric is determined by imposing the physical condition (the axially rotating condition $R_{\hat{r}\hat{\theta}} = 0$) and selecting an appropriate equation of state in the last two steps.

3.3 The inconsistent choices

In this subsection, we demonstrate that arbitrary choices fail to yield a physically consistent geometry by illustrating two examples of metric functions that do not align with axially symmetric rotation in Einstein's theory.

1. Consider the choice $q(x) = x$, $p = 0$. $\Sigma(r, \theta) = r^2 + a^2 \cos^2 \theta$. The metric with this choice becomes,

$$ds^2 = -\frac{\Sigma(r, \theta)\Delta(r)}{\Gamma^2(r)}dt^2 + \Sigma(r, \theta)d\theta^2 + \frac{\Sigma(r, \theta)}{\Delta(r)}dr^2 + \Sigma(r, \theta) \sin^2 \theta \left(d\phi + \frac{a}{\Gamma(r)}dt \right)^2. \quad (34)$$

When we calculate the Ricci tensor, we can easily find that there is no way to set $R_{\hat{r}\hat{\theta}} = -\frac{6a^2r \sin \theta \cos \theta \sqrt{\Delta(r)}}{\Sigma^3(r, \theta)}$ to vanish for all θ unless $a \neq 0$.

2. We next consider the choice $q(x) = x$ and leave $p(x)$ free. Therefore, the metric becomes

$$ds^2 = -\frac{\Sigma(r, \theta)\Delta(r)}{(\Gamma(r) - \dot{p}(x)a^2 \sin^2 \theta)^2} (dt - \dot{p}(x)a \sin^2 \theta d\phi)^2 + \Sigma(r, \theta)d\theta^2 + \frac{\Sigma(r, \theta)}{\Delta(r)}dr^2 + \frac{\Sigma(r, \theta) \sin^2 \theta}{(\Gamma(r) - \dot{p}(x)a^2 \sin^2 \theta)^2} (\Gamma(r)d\phi - a dt)^2. \quad (35)$$

Here, $\Delta(r) = r^2 + a^2 - 2Mr + v(r)$ and $\Gamma(r) \equiv r^2 + a^2 + \tilde{A}(r)$.

The Ricci component $R_{r\theta}$ becomes

$$R_{\hat{r}\hat{\theta}} = \frac{3a^2 \sqrt{\Delta(r)} r \sin 2\theta}{2\rho^6 (\Gamma(r) - a^2 \dot{p}(x) \sin^2 \theta)^2} \left[4a^2 \tilde{A}(r) \dot{p}(x) \sin^2 \theta + 2(a^2 + r^2)^2 - 2(a^2 + r^2 + \tilde{A}(r))^2 + 2(\dot{p}(x) - 1) \left((a^2 + r^2)^2 - p'(x)a^4 \sin^4 \theta \right) + 4\rho^4 \frac{-\ddot{p}(x) (\tilde{A}'(r) + 2r) \cos \theta + 2\dot{p}(x)\tilde{A}'(r)}{8r} \right]. \quad (36)$$

It appears that a unique way which makes $R_{\hat{r}\hat{\theta}} = 0$ for all r and θ must be $\tilde{A}(r) = 0$ and $\dot{p}(x) = 1$. This result reduces the metric into the generalized Kerr solution form (29).

4 Analysis of the new solution

In this section, we analyze the properties of the newly found generalized Kerr solution (33) with metric,

$$ds^2 = -\frac{\Delta(r)}{\Sigma(r, \theta)} (dt - a \sin^2 \theta d\phi)^2 + \frac{\Sigma(r, \theta)}{\Delta(r)} dr^2 + \Sigma(r, \theta) d\theta^2 + \frac{\sin^2 \theta}{\Sigma(r, \theta)} (\Gamma(r) d\phi - a dt)^2. \quad (37)$$

where

$$\Sigma(r, \theta) = r^2 + a^2 \cos^2 \theta, \quad \Delta(r) = r^2 + a^2 - 2Mr + v(r), \quad \Gamma(r) \equiv r^2 + a^2, \quad (38)$$

with $v(r)$ given in Eq. (33).

The energy density of the new solution (33) is

$$\rho = T^{\hat{t}\hat{t}} = -T^{\hat{r}\hat{r}} = \frac{(v(r) - rv'(r))}{8\pi\Sigma^2(r, \theta)} = \frac{v_2 e^{-v_c r^2/2}}{8\pi\Sigma^2(r, \theta)}, \quad (39)$$

and $p_{\hat{\theta}} = p_{\hat{\phi}} = w_2 \rho = \left(1 + \frac{v_c \Sigma(r, \theta)}{2}\right) \rho$. For the energy density localized, we should set $v_c > 0$. The energy density is positive/negative when $v_2 \gtrless 0$. Therefore, we restrict our interest to the case $v_2 > 0$, satisfying the positive energy condition.

Because v_1 modifies the mass only, we set $v_1 = 0$ so that the ADM mass of the black hole becomes just M . Then,

$$\Delta(r) = r^2 - 2Mr + a^2 + v_2 \bar{\Delta}(\sqrt{v_c} r); \quad \bar{\Delta}(y) \equiv e^{-y^2/2} + \sqrt{\frac{\pi y^2}{2}} \left(\operatorname{erf}\left(\frac{|y|}{\sqrt{2}}\right) - 1 \right), \quad (40)$$

$$g_{tt} = -\left(1 - \frac{2Mr - v_2 \bar{\Delta}(\sqrt{v_c} r)}{r^2 + a^2 \cos^2 \theta}\right),$$

where $y = \sqrt{v_c} r$.

We now determine the locations of the ergosphere and the event horizon of the rotating black hole. The ergosphere is the region located between the static limit surface and the outer event horizon [60]. The static limit surface is determined at the location $g_{tt} = 0$, while the event horizon corresponds to a Killing horizon [61], which is located where $\Delta(r) = 0$.

The function $\bar{\Delta}(y)$ monotonically decreases from one at $y = 0$ to zero as $y \rightarrow \infty$. Expanding $\Delta(r)$ around $r \sim 0$ and $r \gg v_c, M$, we get

$$\Delta(r) \approx a^2 + v_2 - \left(2M + \sqrt{\frac{\pi}{2}} v_2\right) r + \dots, \quad \Delta(r) \approx r^2 - 2Mr + a^2 + O(r^{-\infty}).$$

Here,

$$\Delta'(r) = 2(r - M) + v_2 \sqrt{\frac{\pi v_c}{2}} \left(\operatorname{erf}\left(\sqrt{\frac{v_c r^2}{2}}\right) - 1 \right).$$

Let us set the radius r_c such that $\Delta'(r_c) = 0$. At this point, we have

$$\Delta(r_c) = a^2 - r_c^2 + v_2 e^{-v_c r_c^2/2}.$$

For an outer horizon to exist, the value of v_2 should be constrained by the condition $v_2 < (r_c^2 - a^2)e^{v_c r_c^2/2}$.

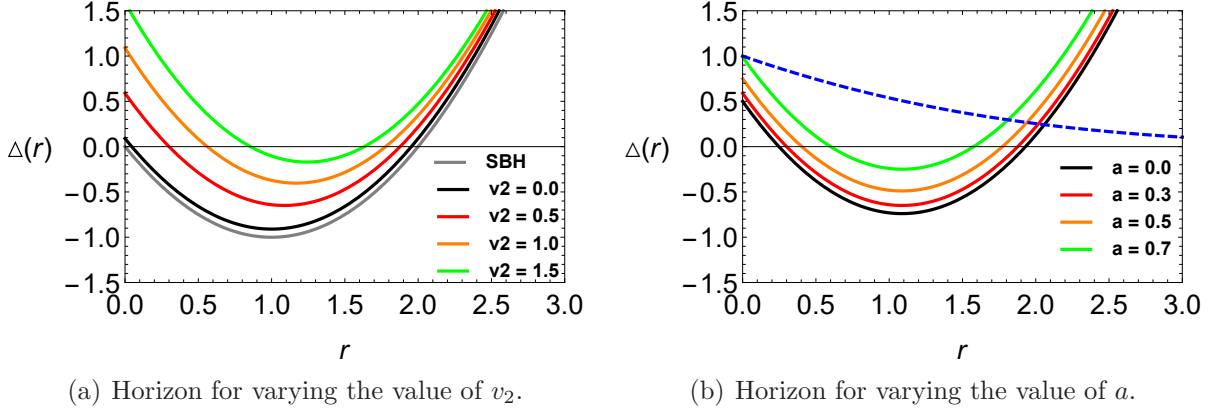


Figure 1: (color online). The characteristic form of the function $\Delta(r)$ for various values of v_2 [L] and a [R], respectively.

Figure 1 illustrates the shape of $\Delta(r)$ as the function of the coordinate r . Figure 1(a) shows the shape of $\Delta(r)$ while varying the value of v_2 , and Fig. 1(b) shows the shape while varying the value of the rotation parameter a . We take $M = 1$ for simplicity. In Fig. 1(a), the gray curve represents a Schwarzschild black hole with $a = 0$ and $v_2 = 0$, while the black curve represents a Kerr black hole with $v_2 = 0$. The red, orange, and green curves represent $\Delta(r)$ with $v_2 = 0.5$, $v_2 = 1.0$, and $v_2 = 1.5$, respectively, with $a = 0.3$. In Fig. 1(b), we take $v_2 = 0.5$. The blue dashed line represents $\bar{\Delta}(\sqrt{v_c}r)$ with $v_c = 0.2$. The black curve represents $\Delta(r)$ with $a = 0.0$, corresponding to the black hole with anisotropic matter. The red, orange, and green curves represent $\Delta(r)$ with $a = 0.3$, $a = 0.5$, and $a = 0.6$, respectively.

Because of the existence of the matter field one can make extremal black hole and a naked singularity before reaching $a = M$. To prevent it, we should restrict the range of a to

$$v_2 \leq (r_c^2 - a^2)e^{v_c r_c^2/2} \quad \rightarrow \quad -\sqrt{\frac{v_2^2 e^{-v_c r_c^2}}{4} + r_c^2} \leq a^2 \leq \sqrt{\frac{v_2^2 e^{-v_c r_c^2}}{4} + r_c^2}.$$

Note that the presence of the $v_2 \bar{\Delta}(y)$ term always increases the value of $\Delta(r)$. Therefore, the radius of the outer horizon r_+ , given by $\Delta(r) = 0$, decreases because of this term. This implies

that the $\bar{\Delta}(y)$ term makes the entropy of the black hole decreases making the Kerr black hole has a maximum entropy.

Given the asymptotic values the mass M and the angular momentum parameter a , the horizon area varies with v_c . This makes the thermodynamic law fails [or depends on the non-asymptotic parameter] to be described by the asymptotic values.

In the $a \rightarrow 0$ limit, this corresponds to a new static black hole geometry with $\omega_r = -1$, and $\omega_\theta = \omega_\phi = 1 + v_c r^2/2$. In other words,

$$\rho^s = \frac{v_2 e^{-v_c r^2/2}}{r^4}, \quad p_r^s = -\rho^s, \quad p_\theta^s = p_\phi^s = \left(1 + \frac{v_c r^2}{2}\right) \rho^s. \quad (41)$$

5 Thermodynamics

We now turn to the thermodynamic properties of this black hole. The surface gravity, which corresponds to the gravitational acceleration on the event horizon as measured by an observer at an asymptotic infinity, is a crucial quantity in black hole thermodynamics. It is constant across the horizon and is directly proportional to the black hole temperature. The black hole entropy has a geometrical interpretation, being proportional to the area of the black hole's horizon. These thermodynamic quantities, as established in [62, 63], are given by

$$T_H = \frac{r_H^2 - a^2 - v_2 e^{-v_c r_H^2/2}}{4\pi r_H (r_H^2 + a^2)}, \quad S = \pi(r_H^2 + a^2) \quad (42)$$

where T_H represents the Hawking temperature and S denotes the entropy.

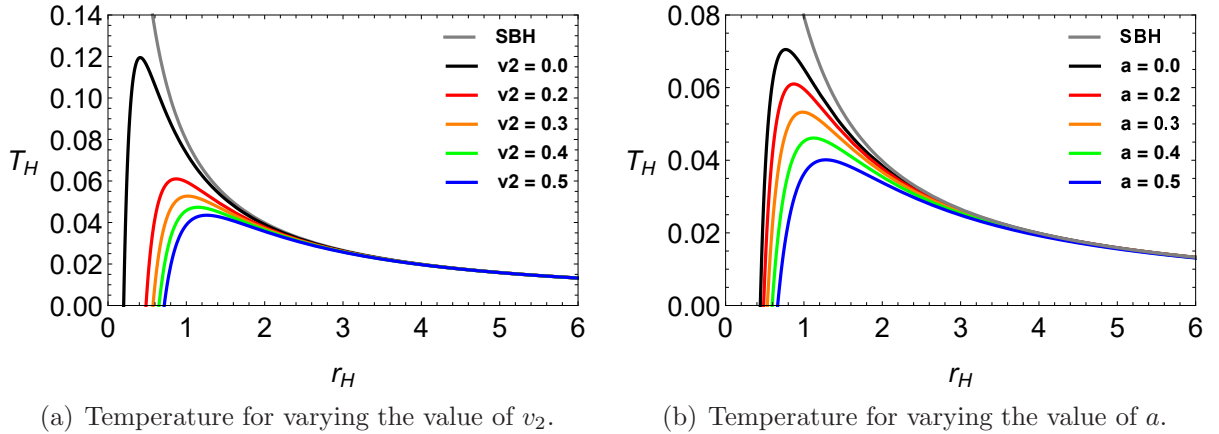


Figure 2: (color online). Temperature as a function of the horizon radius r_H .

Figure 2 illustrates the black hole temperature as a function of the horizon radius r_H for the corresponding black hole solutions. Figure 2(a) shows temperature behavior with varying

values of v_2 , while Fig. 2(b) examines the effect of varying the rotation parameter a . We set $M = 1$ for simplicity. In Fig. 2(a), the grey curve represents the temperature of a Schwarzschild black hole ($a = 0, v_2 = 0$), while the black curve corresponds to the temperature of a Kerr black hole ($a = 0.2, v_2 = 0$). The red, orange, green, and blue curves depict the temperature profiles for $v_2 = 0.2, v_2 = 0.3, v_2 = 0.4$, and $v_2 = 0.5$, respectively. As v_2 increases, the maximum of the temperature shifts to the right and decreases in magnitude. In Fig. (b), the grey curve again corresponds to the temperature of a Schwarzschild black hole ($a = 0, v_2 = 0$), while the black curve represents the temperature of a black hole with anisotropic matter ($a = 0, v_2 = 0.2$). The red, orange, green, and blue curves show the temperature profiles for $a = 0.2, a = 0.3, a = 0.4$, and $a = 0.5$, respectively. As a increases, the maximum temperature similarly shifts to larger r_H and decreases in magnitude.

We now analyze the shape of the temperature curve for $T_H \geq 0$. At large $r_H \gg (a^2 + v_2 e^{-v_2 r_H^2/2})$, the temperature behaves as $T_H \propto r_H^{-1}$, similar to the Schwarzschild black hole. Conversely, for small r_H , the term $-(a^2 + v_2 e^{-v_2 r_H^2/2})$ in the numerator dominates. In this regime, the temperature initially decreases as $T_H \propto -(r_H^{-3})$ transitioning to $T_H \propto -(r_H^{-1})$ as r_H grows slightly larger. As $r_H \rightarrow 0$, T_H diverges to negative infinity. There exists a specific value of r_H where $T_H = 0$, corresponding to an extremal black hole. Additionally, the r_H value at which the black hole temperature reaches its maximum is determined by the condition $dT_H/dr_H = 0$.

Black holes possess hairs [64, 65], such as the mass, angular momentum, and the charge measurable by an asymptotic observer. Using the Smarr relation [66], we construct the Arnowitt-Deser-Misner mass. The potential for the new field is determined by first deriving the mass formula of a static, spherically symmetric black hole:

$$M = 2T_H S + \Phi_1 C_1 + \Phi_2 C_2, \quad (43)$$

where $C_1 = \sqrt{v_2} v_c^{1/4}$, $C_2 = \sqrt{v_2}$, $\Phi_1 = \sqrt{v_2} v_c^{1/4} \sqrt{\frac{\pi}{8}} (\text{erf}(\sqrt{\frac{v_2}{2}} r_H) - 1)$, and $\Phi_2 = \frac{\sqrt{v_2}}{r_H} e^{-\frac{v_2 r_H^2}{2}}$. The new charges C_1 and C_2 , however, cannot be measured asymptotically because the energy density (41) decreases exponentially with r^2 . The Smarr mass of the rotating blackhole (37) is given by

$$M = \frac{1}{2} \left[(M_K + \Phi_1 C_1 + \Phi_2 C_2) + \sqrt{(M_K + \Phi_1 C_1 + \Phi_2 C_2)^2 - 4\Omega_H J (2\Phi_1 C_1 + \Phi_2 C_2)} \right], \quad (44)$$

where $\Omega_H = \frac{a}{r_H^2 + a^2}$, $J = Ma$, $S = \pi(r_H^2 + a^2)$, and $M_K = 2T_H S + 2\Omega_H J$ denotes the mass of the Kerr black hole.

We derive the first law of black hole thermodynamics to establish the differential relationship between the mass, the entropy, the angular momentum, and the new charges of the black hole. The first law takes the form

$$\delta M = \frac{M^2 - \Omega_H J \Phi_1 C_1}{M^2} \left\{ T_H \delta S + \left(1 - \frac{\Phi_1 C_1}{M} \right) \Omega_H \delta J + \left(1 - \frac{\Omega_H J}{M} \right) [2\Phi_1 \delta C_1 + \Phi_2 \delta C_2] \right\}. \quad (45)$$

This relation reduces to the Kerr black hole case, $\delta M_K = T_H \delta S + \Omega_H \delta J$ when $v_2 \rightarrow 0$.

Next, we analyze the specific heat (heat capacity) to evaluate the thermodynamic local stability of the rotating black hole. The heat capacity, $C = T_H \frac{\partial S}{\partial T_H}$, is obtained as follows:

$$C = \frac{2\pi r_H^2 (r_H^2 + a^2) [r_H^2 - a^2 - v_2 e^{-\frac{v_c r_H^2}{2}}]}{a^4 + 4a^2 r_H^2 - r_H^4 + [v_c r_H^2 (r_H^2 + a^2) + 3r_H^2 + a^2] v_2 e^{-\frac{v_c r_H^2}{2}}}. \quad (46)$$

Notice that the numerator is nonnegative when $T_H \geq 0$. Therefore, in this case, the signature of the heat capacity is determined by the value of the denominator. When $v_2 \rightarrow 0$, this expression simplifies to that of the Kerr black hole:

$$C_K = \frac{2\pi r_H^2 (r_H^2 + a^2) (r_H^2 - a^2)}{a^4 + 4a^2 r_H^2 - r_H^4}. \quad (47)$$

When $a \rightarrow 0$, this reduces to that of the static case with corresponding the matter field as follows:

$$C_{\text{gs}} = \frac{2\pi r_H^2 (r_H^2 - v_2 e^{-\frac{v_c r_H^2}{2}})}{-r_H^2 + v_2 (v_c r_H^2 + 3) e^{-\frac{v_c r_H^2}{2}}}.$$

Please compare this result with that of the Schwarzschild.

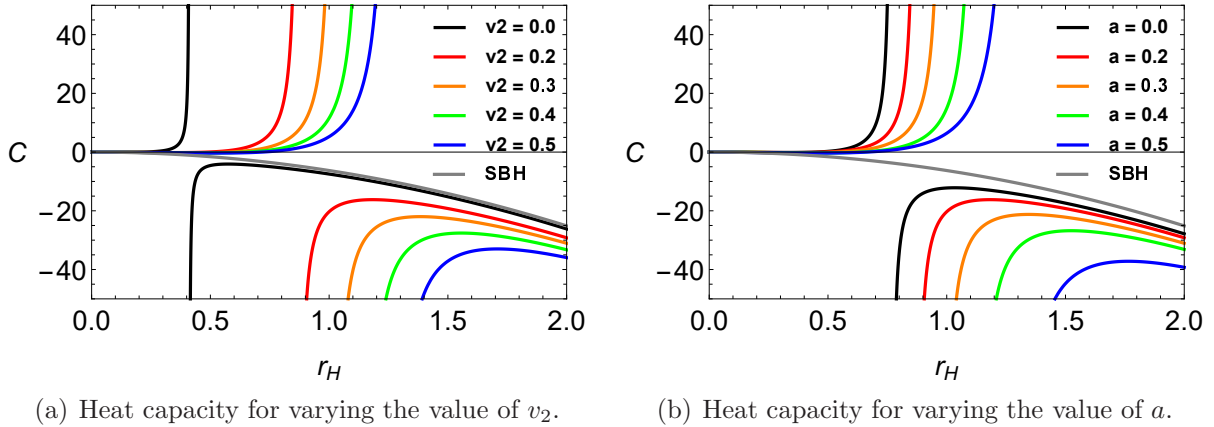


Figure 3: (color online). Heat capacity as a function of the horizon radius r_H .

Figure 3 illustrates the heat capacity as a function of the horizon radius r_H for the black hole solutions. The black hole is locally thermodynamically stable when the heat capacity is positive and unstable when it is negative. The singular point in each Figure corresponds to the convex upward point of the respective curve in Fig. 2, where $|\partial r_H / \partial T_H| \rightarrow \infty$. Figure 3(a) depicts the heat capacity for varying value of v_2 , while Fig. 3(b) examines the effect of different

rotation parameter a values. In Fig. 3(a), the grey curve represents the heat capacity of a Schwarzschild black hole ($a = 0, v_2 = 0$). The black curve corresponds to the heat capacity of the Kerr black hole with ($a = 0.2, v_2 = 0$). The red, orange, green, and blue curves represent the heat capacity with $v_2 = 0.2, v_2 = 0.3, v_2 = 0.4$, and $v_2 = 0.5$, respectively. In Fig. 3(b), the grey curve again corresponds to the Schwarzschild black hole. The black curve represents a black hole with the anisotropic matter with ($a = 0, v_2 = 0.2$). The red, orange, green, and blue curves illustrate the heat capacity for $a = 0.2, a = 0.3, a = 0.4$, and $a = 0.5$, respectively.

6 Summary and discussions

We investigated the Newman-Janis (NJ) algorithm in a general context as a method for constructing rotating geometries from static ones. Our analysis demonstrated that the NJ algorithm serves as a powerful mathematical tool, simplifying the structure of general rotating metrics by imposing basic physical constraints. Through a detailed examination of the black hole metric to which the NJ algorithm is applied, we derived a new rotating black hole solution in a quite general form.

While the traditional approach applies the NJ algorithm to a static, spherically symmetric black hole to obtain a rotating counterpart, our method first derives the rotating black hole geometry directly through an analysis of the NJ algorithm. We then work backward to retrieve the corresponding spherically symmetric black hole solution. One key requirement for a well-defined rotating black hole solution is that the Einstein tensor component $R_{\hat{r}\hat{\theta}}$ should vanish in an orthonormal basis, a condition that our newly derived metric satisfies. The NJ algorithm is particularly well-defined when applied to static, spherically symmetric black holes with $f(r) = g(r)$.

However, obtaining a rotating black hole solution becomes more challenging when the NJ algorithm is not well-defined for a given geometry. This issue arises, for instance, when $f(r) \neq g(r)$, when a cosmological constant is present, or when the black hole is immersed in a magnetic field. In the case of $f(r) \neq g(r)$, the standard approach is to solve Einstein's equations directly by using a metric ansatz, and verify whether $R_{\hat{r}\hat{\theta}} = 0$. An example of this method applied within the NJ algorithm framework can be found in [67]. For black holes with a cosmological constant, one may follow Carter's method [68], while black holes immersed in the magnetic field require analysis based on Ernst spacetime [69, 70].

The energy budget of our Universe is composed of approximately 5% ordinary matter and 95% dark energy and dark matter [71]. Recent astrophysical and cosmological precision observations have intensified the trend toward studying cosmological and astrophysical models involving dark energy and dark matter [72, 73, 74, 75]. These phenomena have motivated us to study black holes that coexist with matter fields, with the goal of understanding and explaining their nature.

Notably, we found that the geometry of the rotating black hole solution is not uniquely determined by asymptotic parameters such as mass, charge, angular momentum, or any other

gauge charges. Specifically, a matter field exists near the black hole horizon, with its density decaying not later than exponentially at large distances. This solution, therefore, challenges the no-hair conjecture and suggests the existence of a new form of black hole "hair" that remains undetectable in the asymptotic region. Investigating the properties of such a matter field in curved spacetime would be an intriguing direction for future research. An alternative, indirect approach is to analyze black hole thermodynamics by defining a new charge associated with this field and identifying the corresponding potential.

We analyzed black hole thermodynamics, defining the charge for the new field and identifying the corresponding potential. This allowed us to derive the Smarr relation and the first law of black hole thermodynamics. This approach indirectly demonstrates the existence of the new hair. Additionally, we analyzed the black hole temperature and heat capacity, which reveals the thermodynamic local stability of the black hole.

Acknowledgments

We are grateful to Wontae Kim and Stefano Scopel for their hospitality during our visit to the Workshop on Cosmology and Quantum Spacetime (CQUeST 2024), and Inyong Cho to the workshop on How to use AI in Astrophysics Theory. H.-C. Kim (RS-2023-00208047) and W. Lee (RS-2022-NR075087, CQUeST: RS-2020-NR049598) were supported by Basic Science Research Program through the National Research Foundation of Korea funded by the Ministry of Education.

References

- [1] K. Akiyama *et al.* [Event Horizon Telescope Collaboration], *Astrophys. J.* **875**, no. 1, L1 (2019).
- [2] K. Akiyama *et al.* [Event Horizon Telescope Collaboration], *Astrophys. J.* **875**, no. 1, L4 (2019).
- [3] K. Akiyama *et al.* [Event Horizon Telescope Collaboration], *Astrophys. J.* **875**, no. 1, L5 (2019).
- [4] B. P. Abbott *et al.* [LIGO Scientific and Virgo Collaborations], *Phys. Rev. Lett.* **116**, no. 22, 221101 (2016) [arXiv:1602.03841 [gr-qc]].
- [5] B. P. Abbott *et al.* [LIGO Scientific and Virgo Collaborations], *Phys. Rev. Lett.* **116**, no. 24, 241103 (2016) [arXiv:1606.04855 [gr-qc]].
- [6] B. P. Abbott *et al.* [LIGO Scientific and VIRGO Collaborations], *Phys. Rev. Lett.* **118**, no. 22, 221101 (2017) Erratum: [*Phys. Rev. Lett.* **121**, no. 12, 129901 (2018)] [arXiv:1706.01812 [gr-qc]].

- [7] Y. B. Bae, Y. H. Hyun and G. Kang, Phys. Rev. Lett. **132**, no.26, 261401 (2024) [arXiv:2310.18686 [gr-qc]].
- [8] R. P. Kerr, Phys. Rev. Lett. **11**, 237 (1963).
- [9] E. T. Newman, R. Couch, K. Chinnapared, A. Exton, A. Prakash and R. Torrence, J. Math. Phys. **6**, 918 (1965).
- [10] E. T. Newman and A. I. Janis, J. Math. Phys. **6**, 915 (1965).
- [11] S. P. Drake and P. Szekeres, Gen. Rel. Grav. **32**, 445 (2000) [gr-qc/9807001].
- [12] M. Azreg-Ainou, Phys. Rev. D **90**, no. 6, 064041 (2014) [arXiv:1405.2569 [gr-qc]].
- [13] T. Adamo and E. T. Newman, Scholarpedia **9**, 31791 (2014) [arXiv:1410.6626 [gr-qc]].
- [14] B. Toshmatov, Z. Stuchlik and B. Ahmedov, Eur. Phys. J. Plus **132**, no. 2, 98 (2017) [arXiv:1512.01498 [gr-qc]].
- [15] Z. Xu and J. Wang, Phys. Rev. D **95**, no. 6, 064015 (2017) [arXiv:1609.02045 [gr-qc]].
- [16] H. C. Kim, B. H. Lee, W. Lee and Y. Lee, Phys. Rev. D **101**, no.6, 064067 (2020) [arXiv:1912.09709 [gr-qc]].
- [17] H. C. Kim, B. H. Lee, W. Lee and Y. Lee, AIP Conf. Proc. **2874**, no.1, 020008 (2024) [arXiv:2112.04131 [gr-qc]].
- [18] A. I. Janis and E. T. Newman, J. Math. Phys. **6**, 902-914 (1965).
- [19] H. Erbin, Gen. Rel. Grav. **47**, 19 (2015) [arXiv:1410.2602 [gr-qc]].
- [20] A. Sen, Phys. Rev. Lett. **69**, 1006-1009 (1992) [arXiv:hep-th/9204046 [hep-th]].
- [21] H. Kim, Phys. Rev. D **60**, 024001 (1999) [arXiv:gr-qc/9811012 [gr-qc]].
- [22] G. W. Gibbons, H. Lu, D. N. Page and C. N. Pope, Phys. Rev. Lett. **93**, 171102 (2004) [hep-th/0409155].
- [23] C. Bambi and L. Modesto, Phys. Lett. B **721**, 329 (2013) [arXiv:1302.6075 [gr-qc]].
- [24] C. A. R. Herdeiro and E. Radu, Phys. Rev. Lett. **112**, 221101 (2014) [arXiv:1403.2757 [gr-qc]].
- [25] S. Brahma, C. Y. Chen and D. h. Yeom, Phys. Rev. Lett. **126**, no.18, 181301 (2021) [arXiv:2012.08785 [gr-qc]].
- [26] A. Simpson and M. Visser, JCAP **03**, no.03, 011 (2022) [arXiv:2111.12329 [gr-qc]].

- [27] D. O. Devecioglu and M. I. Park, Eur. Phys. J. C **84**, no.8, 852 (2024) [arXiv:2402.02253 [hep-th]].
- [28] H. Stephani, D. Kramer, M. A. H. MacCallum, C. Hoenselaers and E. Herlt, Cambridge Univ. Press, 2003, ISBN 978-0-521-46702-5, 978-0-511-05917-9
- [29] M. S. R. Delgaty and K. Lake, Comput. Phys. Commun. **115**, 395-415 (1998) [arXiv:gr-qc/9809013 [gr-qc]].
- [30] I. Semiz, Rev. Math. Phys. **23**, 865-882 (2011) [arXiv:0810.0634 [gr-qc]].
- [31] M. Ruderman, Ann. Rev. Astron. Astrophys. **10**, 427-476 (1972)
- [32] L. Herrera and J. Jimenez, J. Math. Phys. **23**, 2339 (1982).
- [33] L. Herrera and N. O. Santos, Phys. Rept. **286** (1997) 53.
- [34] R. L. Bowers and E. P. T. Liang, Astrophys. J. **188** (1974) 657.
- [35] J. J. Matese and P. G. Whitman, Phys. Rev. D **22** (1980) 1270.
- [36] M. K. Mak and T. Harko, Proc. Roy. Soc. Lond. A **459** (2003) 393 [gr-qc/0110103].
- [37] S. Thirukkanesh and S. D. Maharaj, Class. Quant. Grav. **25** (2008) 235001 [arXiv:0810.3809 [gr-qc]].
- [38] B. V. Ivanov, Phys. Rev. D **65** (2002) 104011 [gr-qc/0201090].
- [39] V. Varela, F. Rahaman, S. Ray, K. Chakraborty and M. Kalam, Phys. Rev. D **82** (2010) 044052 [arXiv:1004.2165 [gr-qc]].
- [40] I. Cho and H. C. Kim, Chin. Phys. C **43**, no. 2, 025101 (2019) [arXiv:1703.01103 [gr-qc]].
- [41] H. C. Kim and Y. Lee, Eur. Phys. J. C **79** (2019) no.8, 679 [arXiv:1901.03148 [hep-th]].
- [42] J. D. Bekenstein, Phys. Rev. Lett. **28**, 452-455 (1972).
- [43] J. D. Bekenstein, Phys. Rev. D **51**, no.12, R6608 (1995)
- [44] C. A. R. Herdeiro and E. Radu, Int. J. Mod. Phys. D **24**, no.09, 1542014 (2015) [arXiv:1504.08209 [gr-qc]].
- [45] G. Antoniou, A. Bakopoulos and P. Kanti, Phys. Rev. Lett. **120**, no.13, 131102 (2018) [arXiv:1711.03390 [hep-th]].
- [46] D. D. Doneva and S. S. Yazadjiev, Phys. Rev. Lett. **120**, no.13, 131103 (2018) [arXiv:1711.01187 [gr-qc]].

- [47] B. H. Lee, W. Lee and D. Ro, Phys. Rev. D **99**, no.2, 024002 (2019) [arXiv:1809.05653 [gr-qc]].
- [48] M. Minamitsuji and H. Motohashi, Phys. Rev. D **98**, no.8, 084027 (2018) [arXiv:1809.06611 [gr-qc]].
- [49] D. C. Zou and Y. S. Myung, Phys. Rev. D **101**, no.8, 084021 (2020) [arXiv:2001.01351 [gr-qc]].
- [50] A. Papageorgiou, C. Park and M. Park, Phys. Rev. D **106**, no.8, 084024 (2022) [arXiv:2205.00907 [hep-th]].
- [51] B. H. Lee, H. Lee and W. Lee, AIP Conf. Proc. **2874**, no.1, 020011 (2024) [arXiv:2111.13380 [gr-qc]].
- [52] B. A. Campbell, M. J. Duncan, N. Kaloper and K. A. Olive, Phys. Lett. B **251**, 34-38 (1990).
- [53] S. R. Coleman, J. Preskill and F. Wilczek, Phys. Rev. Lett. **67**, 1975-1978 (1991).
- [54] S. R. Coleman, J. Preskill and F. Wilczek, Nucl. Phys. B **378**, 175-246 (1992) [arXiv:hep-th/9201059 [hep-th]].
- [55] V. P. Frolov and I. D. Novikov, *Black hole physics: Basic concepts and new developments*, Kluwer Academic Publishers, Dordrecht, 1998.
- [56] R. H. Boyer and R. W. Lindquist, J. Math. Phys. **8**, 265 (1967).
- [57] M. Azreg-Ainou, Phys. Lett. B **730**, 95 (2014) [arXiv:1401.0787 [gr-qc]].
- [58] T. Jacobson, Class. Quant. Grav. **24**, 5717-5719 (2007) [arXiv:0707.3222 [gr-qc]].
- [59] R. M. Teixeira Filho and V. B. Bezerra, Phys. Rev. D **64**, 084009 (2001).
- [60] R. Ruffini and J. A. Wheeler, *Relativistic Cosmology And Space Platforms*, PRINT-70-2077.
- [61] B. Carter, J. Math. Phys. **10**, 70 (1969).
- [62] J. D. Bekenstein, Phys. Rev. D **7**, 2333-2346 (1973).
- [63] S. W. Hawking, Commun. Math. Phys. **43**, 199-220 (1975) [erratum: Commun. Math. Phys. **46**, 206 (1976)].
- [64] R. Ruffini and J. A. Wheeler, Phys. Today **24**, no. 1, 30 (1971).
- [65] J. M. Bardeen, B. Carter and S. W. Hawking, Commun. Math. Phys. **31**, 161 (1973).

- [66] L. Smarr, Phys. Rev. Lett. **30**, 71 (1973) Erratum: [Phys. Rev. Lett. **30**, 521 (1973)].
- [67] H. C. Kim, S. W. Kim, B. H. Lee and W. Lee, [arXiv:2405.10013 [gr-qc]].
- [68] B. Carter, “Black holes equilibrium states,” in Black Holes, edited by C. De Witt and B. S. De Witt (Gordon and Breach, New York, 1973).
- [69] F. J. Ernst, J. Math. Phys. **17**, no.1, 54-56 (1976).
- [70] F. J. Ernst and W. J. Wild, J. Math. Phys. **17**, no.2, 182 (1976).
- [71] N. Aghanim *et al.* [Planck], Astron. Astrophys. **641**, A1 (2020) [arXiv:1807.06205 [astro-ph.CO]].
- [72] S. M. Ko, J. H. Park and M. Suh, JCAP **06**, 002 (2017) [arXiv:1606.09307 [hep-th]].
- [73] J. W. Lee, H. C. Kim and J. Lee, Phys. Lett. B **795**, 206-210 (2019) [arXiv:1901.00305 [astro-ph.GA]].
- [74] A. Biswas, A. Kar, B. H. Lee, H. Lee, W. Lee, S. Scopel, L. Velasco-Sevilla and L. Yin, JCAP **08**, 024 (2023) [arXiv:2303.05813 [hep-ph]].
- [75] J. Lee and Y. Yun, [arXiv:2502.19880 [gr-qc]].